

Relationship Between ^{18}F -Flortaucipir Uptake and Histologic Lesion Types in 4-Repeat Tauopathies

Keith A. Josephs¹, Nirubol Tosakulwong², Stephen D. Weigand², Marina Buciu¹, Val J. Lowe³, Dennis W. Dickson⁴, and Jennifer L. Whitwell³

¹Department of Neurology, Mayo Clinic, Rochester, Minnesota; ²Department of Health Sciences Research, Mayo Clinic, Rochester, Minnesota; ³Department of Radiology, Mayo Clinic, Rochester, Minnesota; and ⁴Department of Neuroscience, Mayo Clinic, Rochester, Minnesota

Progressive supranuclear palsy (PSP) and corticobasal degeneration (CBD) are 4-repeat (4R) tauopathies with overlapping, but also morphologically distinct, tau immunoreactive lesions that vary in count by brain region. ^{18}F -flortaucipir PET uptake has been reported to correlate with overall tau burden, and—in 1 CBD case—to have greater affinity to threads than tangles. We determined whether ^{18}F -flortaucipir uptake is associated with histologic lesion type in 4R tauopathies. **Methods:** We performed semiquantitative regional lesion counts on pretangles/neurofibrillary tangles, threads, oligodendroglial coiled bodies, tufted astrocytes, and astrocytic plaques in 29 cases of autopsy-confirmed 4R tauopathy (PSP, 16; CBD, 13). Regression models were used for statistical analyses. **Results:** ^{18}F -flortaucipir uptake marginally correlated with threads in the precentral cortex ($P = 0.04$) and with astrocytic lesions in the red nucleus ($P = 0.05$). **Conclusion:** The findings do not support ^{18}F -flortaucipir's having differential affinity to any 4R tau lesion type.

Key Words: progressive supranuclear palsy; corticobasal degeneration; PET; pathology; AV-1451

J Nucl Med 2022; 63:931–935
DOI: 10.2967/jnumed.121.262685

Progressive supranuclear palsy (PSP) and corticobasal degeneration (CBD) are 4-repeat (4R) tauopathies that are pathologically characterized by overlapping lesion distributions and morphologies, as well as distinct tau immunoreactive lesions that vary in count (amount), depending on which brain region is assessed (1,2). Both PSP and CBD are characterized by the presence of pretangles/neurofibrillary tangles (neuronal), oligodendroglial coiled bodies (glial), and threads (neuronal > glial), whereas PSP has only tufted astrocytes (glial) and CBD has only astrocytic plaques (glial) (1,2). CBD has a predominantly corticostriatal distribution of lesion burden with less involvement of brain stem regions, whereas PSP has a predominantly brain stem distribution of lesion burden.

^{18}F -flortaucipir (also known as ^{18}F -AV-1451 and ^{18}F -T807) is a small indole ligand that is made with a radioactive fluorine isotope that robustly binds to paired helical filament (3R + 4R) tau that occurs in Alzheimer disease brains (3,4). Therefore, ^{18}F -flortaucipir

is considered an antemortem biomarker for visualizing underlying paired helical filament tau in Alzheimer disease. Regional ^{18}F -flortaucipir PET uptake has been described in clinical syndromes suspected to have underlying 4R tau (5) and in a few autopsied cases of 4R tauopathies where uptake was reported to correlate with histopathologic tau lesion burden (6,7). In these individual cases, a correlation was identified by assessing the relationship between ^{18}F -flortaucipir uptake across multiple brain regions and histopathologic tau lesion count, whereby count was treated as a single variable combining all lesion types. ^{18}F -flortaucipir uptake has been shown to have greater affinity for threads than for tangles, again across multiple brain regions, in a single CBD case (7). More recently, in an autopsied case series we found correlations between ^{18}F -flortaucipir and histologic tau to be selective and limited to only a few brain regions, particularly the red nucleus of the midbrain (8). We did not assess lesion type, however.

Given these findings, we aimed to investigate in a relatively large autopsy-confirmed cohort of PSP and CBD cases with antemortem ^{18}F -flortaucipir whether ligand uptake does indeed show evidence of differential affinity for threads and, if so, whether such a relationship would be region-specific or whether different regions would show different lesion affinities. We hypothesize that ^{18}F -flortaucipir uptake would correlate to overall tau burden in the red nucleus but not to any single specific lesion since all lesion types are represented in the red nucleus in CBD or PSP.

MATERIALS AND METHODS

Participant Cohort

All participants were prospectively recruited by the Neurodegenerative Research Group at Mayo Clinic, Minnesota, as part of a National Institutes of Health–funded grant and met 2 inclusion criteria: completion of antemortem volumetric head MRI, ^{18}F -flortaucipir PET, and Pittsburgh compound B PET; and a brain autopsy with a pathologic diagnosis of PSP or CBD between April 7, 2016, and April 6, 2021.

The study was approved by the Mayo Clinic Institutional Review Board, and all patients gave written informed consent to participate in the study.

Neuropathologic Evaluation and Diagnosis

All patients had a standardized neuropathologic evaluation in accordance with accepted published methodologies (9), including immunohistochemistry to detect 4R tau immunoreactive lesions using an antibody to phospho-tau (CP13; 1:1,000; IgG1 to phospho-serine 202, gift from the late Peter Davies, Feinstein Institute). PSP and CBD pathologic diagnoses were rendered according to published criteria

Received Jul. 12, 2021; revision accepted Sep. 21, 2021.
For correspondence or reprints, contact Keith A. Josephs (josephs.keith@mayo.edu).

Published online Sep. 23, 2021.

COPYRIGHT © 2022 by the Society of Nuclear Medicine and Molecular Imaging.

(1,2). PSP was diagnosed if there were globose neurofibrillary tangles, tufted astrocytes, and oligodendroglial coiled bodies in cardinal nuclei (2), whereas CBD was diagnosed if there were balloon neurons, as well as tau-specific lesions of pretangles, astrocytic plaques, and threads in cardinal nuclei (1). Additional pathologic findings were documented as previously described (8).

Semiquantitative 4R Tau Lesion Count

We assessed the burden (lesion count) of tau-specific lesions with anti-CP13 antibodies and immunohistochemistry. Lesions were counted by a single neuropathologist in the cerebellar dentate, midbrain tegmentum, substantia nigra, red nucleus, subthalamic nucleus, ventral thalamus, globus pallidus, striatum, superior frontal cortex, and precentral (motor) cortex. For each of these 10 regions, we determined lesion count for pretangles/neurofibrillary tangles, coiled bodies, tufted astrocytes (PSP only), and astrocytic plaques (CBD only) (Fig. 1) scored using a semiquantitative 4-point scale as follows: 0, absent lesions; 1+, few lesions (1–3 per $\times 200$ field); 2+, moderate number of lesions (4–6 per $\times 200$ field); and 3+, frequent number of lesions (7 or more per $\times 200$ field). The density of neuropil threads was also graded on the same 0–3 scale (Fig. 1). This semiquantitative scale was published in 2006, in an article that displays specific exemplars or representative images for each score, for 3 of the lesions analyzed in this study (10).

PET Analysis

All participants underwent a standardized MRI protocol at 3 T that included a magnetization-prepared rapid gradient-echo (MPRAGE) sequence. ^{18}F -flortaucipir and Pittsburgh compound B PET scans were acquired using a PET/CT scanner (Discovery MR750; GE Healthcare) (11). All MPRAGE scans were normalized to the Mayo Clinic Adult

Lifespan Template and segmented via unified segmentation with Mayo Clinic Adult Lifespan Template priors or settings. ^{18}F -flortaucipir images were coregistered to the MPRAGE using 6°-of-freedom registration in SPM12. Region-level data were calculated for the MPRAGE-space ^{18}F -flortaucipir PET to allow for correlations with histopathology. Our analysis was performed on the hemisphere to match the hemisphere sampled at autopsy. To assess for correlations between ^{18}F -flortaucipir uptake and histology lesion counts, we selected regions of interest that matched the regions assessed at autopsy. The Mayo Clinic Adult Lifespan Template atlas was used to assess uptake in the superior frontal, motor cortex, thalamus, globus pallidus, and striatum; the Deep Brain Stimulation Intrinsic Template (12) atlas for uptake in the substantia nigra, subthalamic nucleus, and red nucleus; and an in-house—developed atlas for the midbrain and cerebellar dentate, as previously described (5). All regional uptake values were divided by median uptake in the cerebellar crus gray matter to calculate SUV ratio (SUVr). A 2-compartment partial-volume correction was performed (13). The analyses were also repeated using PET data without partial-volume correction. Regional volumes were also calculated from the MPRAGE for the same 10 regions to allow for the assessment of potential confounding effects due to atrophy. Global Pittsburgh compound B SUVrs were calculated as previously described (14) and converted to centiloid units as follows: centiloid = $100 \times [(-0.1620 + 0.9467 \times \text{global Pittsburgh compound B SUVr}) - 1.009]/1.067$ (15).

Statistical Analysis

For each region, we fit a linear regression model with log-transformed tau PET SUVr as the response and semiquantitative tau lesion burden scores as the predictors of interest. We incorporated the lesion count scores in several ways to have a more complete understanding of their effects. In our first approach, we included the scores for the 4 lesion types as 4 separate predictors in the model. In the second approach, we included the sum of the scores of the preneurofibrillary or neurofibrillary tangles plus tau threads as a first predictor and the sum of the scores of coiled bodies and astrocytic lesions as a second predictor. In the last approach, we summed all 4 semiquantitative scores to form a single numeric composite. We used the natural logarithm as the response in these models to reduce skew, maintain the regression assumption of constant variance, and allow an interpretation of the effect of tau burden in terms of percentage difference in PET uptake. All models included time from PET scan to death, age at death, and total intracranial volume as covariates.

RESULTS

We identified 29 cases that met our inclusion criteria of having had an antemortem ^{18}F -flortaucipir PET scan, died with autopsy, and had a pathologic diagnosis of PSP ($n = 16$) or CBD ($n = 13$). Table 1 shows the demographic characteristics of all 29, as well as differences between those with PSP and those with CBD. Those with CBD were younger by an average of 3 y at the time of the scan and were more likely to have aging-related tau astrogliopathy and argyrophilic grains disease at death as secondary pathologies.

The distribution of pathology across regions is shown in Figure 2. The only associations between tau pathology and ^{18}F -flortaucipir uptake that reached marginal significance were between ^{18}F -flortaucipir uptake and total lesion burden in the red nucleus ($P = 0.05$) and the precentral gyrus ($P = 0.04$) (Fig. 3). The association in the red nucleus was driven mainly by glial lesions, that is, astrocytic lesions, whereas the association in the precentral gyrus was driven by neuronal lesions, that is, threads. We also observed a trend for the subthalamic nucleus to show relationships like those of the red nucleus. The results remained the same using PET data without partial-volume

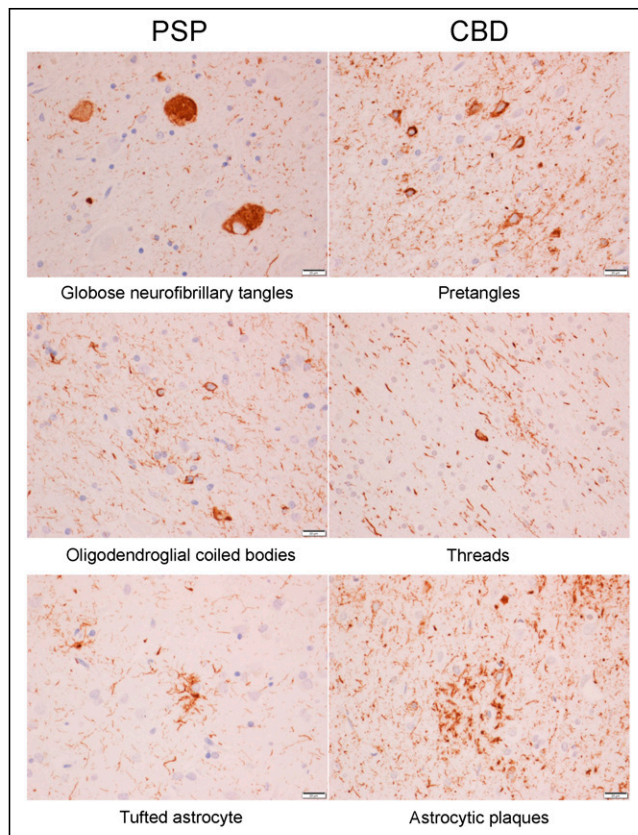


FIGURE 1. Different types of 4R tau lesions in PSP and CBD. Bar at lower right of each image indicates magnification level.

TABLE 1
Participant Characteristics

Characteristic	All (n = 29)	CBD (n = 13)	PSP (n = 16)	P
Female	12 (41%)	6 (46%)	6 (38%)	0.72
Education (y)	16 (12, 16)	14 (12, 16)	16 (14, 16)	0.29
Age at death (y)	74 (68, 78)	68 (60, 74)	78 (69, 80)	0.009
Age at tau PET (y)	70 (67, 77)	67 (58, 73)	76 (68, 78)	0.02
Tau PET to death (y)	1.3 (0.93, 2.43)	1.2 (0.93, 1.50)	1.4 (1.0, 2.5)	0.71
APOE carrier	3 (12%)	1 (9%)	2 (14%)	>0.99
22	0 (0%)	0 (0%)	0 (0%)	
23	5 (20%)	2 (18%)	3 (21%)	
33	17 (68%)	8 (73%)	9 (64%)	
34	2 (8%)	0 (0%)	2 (14%)	
44	1 (4%)	1 (9%)	0 (0%)	
NFT-positive	27 (93%)	12 (92%)	15 (94%)	>0.99
Braak NFT stage				0.18
1	4 (15%)	0 (0%)	4 (29%)	
2	5 (19%)	4 (33%)	1 (7%)	
3	9 (35%)	5 (42%)	4 (29%)	
4	8 (31%)	3 (25%)	5 (36%)	
5	0 (0%)	0 (0%)	0 (0%)	
6	0 (0%)	0 (0%)	0 (0%)	
ARTAG-positive	18 (64%)	11 (85%)	7 (47%)	0.05
Grain disease-positive	13 (46%)	7 (54%)	6 (40%)	0.71
MoCA	18 (10, 22)	12 (7, 20)	18 (16, 23)	0.18
UPDRS III	56 (44, 72)	53 (44, 72)	59 (47, 72)	0.61
PiB PET SUVRs	1.43 (1.37, 1.75)	1.41 (1.37, 1.44)	1.73 (1.37, 1.93)	0.30
a β centiloid	17 (12, 46)	16 (12, 18)	44 (12, 61)	0.30

APOE = apolipoprotein E; NFT = neurofibrillary tangle; ARTAG = aging-related tau astroglipathy; MoCA = Montreal Cognitive Assessment; UPDRS III = Movement Disorders Society sponsored revision of Unified Parkinson Disease Rating Scale; PiB = Pittsburgh compound B; A β = β -amyloid.

Data are median and interquartile range or number and percentage. *P* values are from Fisher exact test or Wilcoxon rank sum test when appropriate.

correction (Supplemental Fig. 1; supplemental materials are available at <http://jnm.snnjournals.org>). There was no evidence that volumes differed by ¹⁸F-flortaucipir uptake or that volumes were smaller in those with low uptake (Fig. 4).

DISCUSSION

In this study of 29 cases of autopsied PSP and CBD (4R tauopathies) with antemortem ¹⁸F-flortaucipir imaging, we found marginal associations between ligand uptake and histopathologic lesion count when combining all lesion types in 2 regions only, the red nucleus and the precentral gyrus. The association in the precentral gyrus appeared to be more related to threads, whereas in the red nucleus it appeared to be related to astrocytic lesions.

It is well known that ¹⁸F-flortaucipir binds strongly to tau in Alzheimer disease but not to tau in PSP and CBD. Two hypotheses for this differential affinity include binding affinity's being related to the tau isoform or to the structure of the tau filaments. That is, differential binding of ¹⁸F-flortaucipir is related to the ligand's having stronger

affinity for tau enriched with mixed 3R + 4R tau isoforms than for tau enriched with predominantly 4R tau isoforms (3) or to ¹⁸F-flortaucipir's binding better to paired helical filamentous tau that characterizes the tau filaments in Alzheimer disease (3). It is also possible, however, that differential binding is related to ultrastructural differences between the tau in Alzheimer disease and the tau in 4R tauopathies. A recent cryoelectron microscopic study and another study showed that 4R tauopathies have unique tau aggregated ultrastructural confirmations that differ from that of Alzheimer disease (16,17).

Neither threads nor astrocytic lesions in PSP and CBD are enriched with mixed 3R + 4R tau or are characterized by paired helical filaments. The marginal correlations identified in the 2 regions in this study confirm our previous findings (8). However, they do not support ¹⁸F-flortaucipir's having differential affinity for any one lesion type. We are not able to biologically elucidate why there were correlations of significance between ligand uptake and those 2 specific lesion types in red nucleus and precentral gyrus. One explanation could be that there is some Alzheimer (3R + 4R paired helical filament) tau that is codeposited with 4R tau in these 2 regions. An argument against this

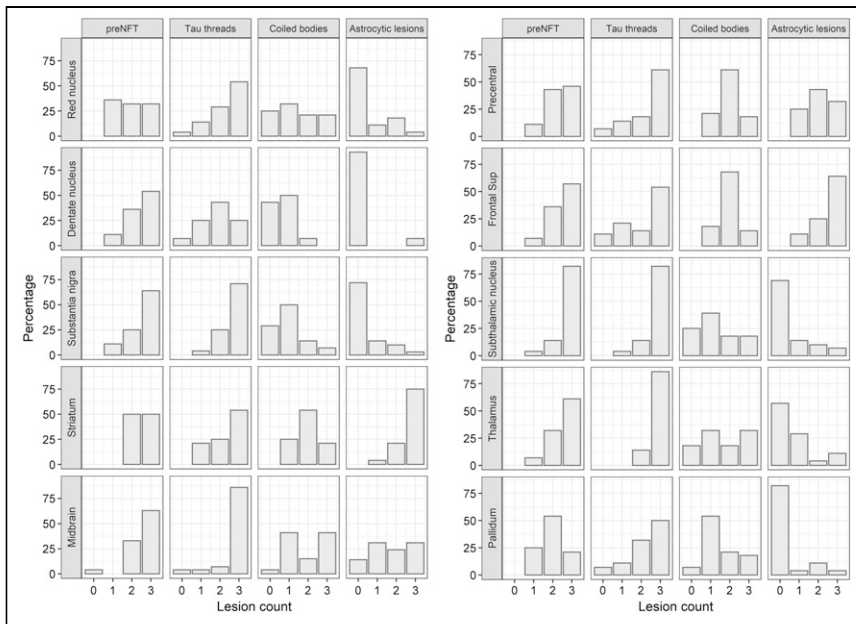


FIGURE 2. Histograms showing distribution of lesion count scores across cases for each region and each tau lesion type.

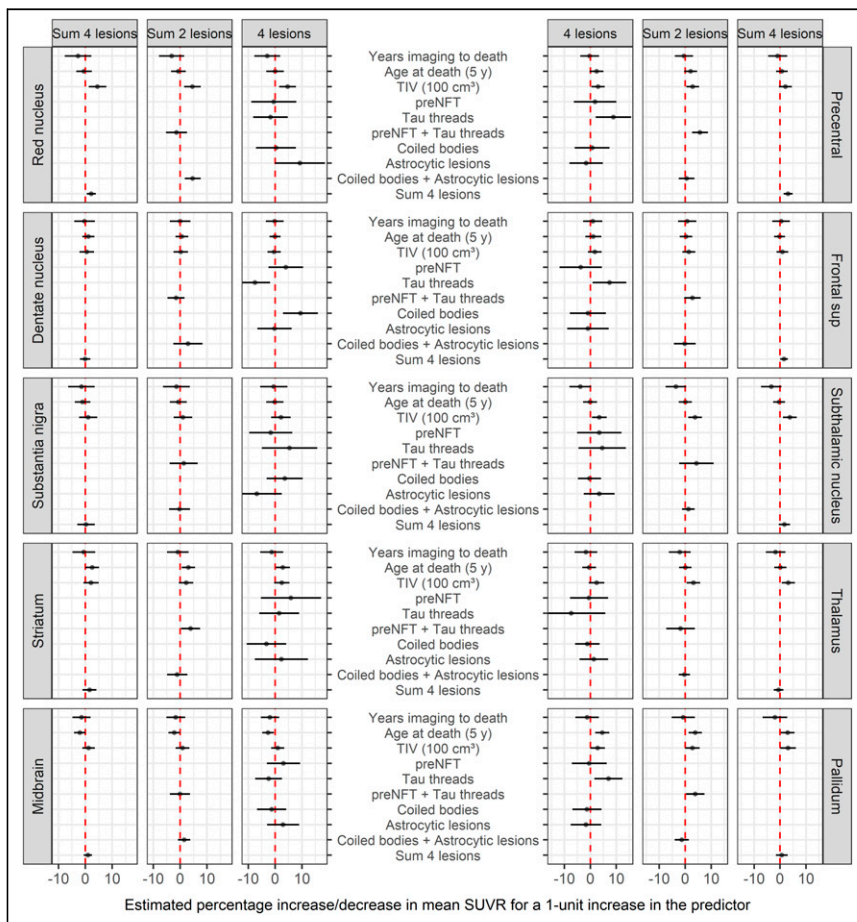


FIGURE 3. Relationships between ^{18}F -flortaucipir uptake (SUVR) and lesion type, adjusting for time from imaging to death, age at death, and total intracranial volume. NFT = neurofibrillary tangle; TIV = total intracranial volume.

explanation is that the highest Braak neurofibrillary tangle stage in any of the 29 patients in this study was IV (most were Braak neurofibrillary tangle stages 0–III), and hence there was no Alzheimer-type tau in any of the 10 regions analyzed in this study. Furthermore, we have previously shown that ^{18}F -flortaucipir PET is not sensitive to low levels of tau pathology (8). Another is that we are observing correlations that are influenced by regional off-target binding. This latter explanation is supported by previous studies that have found evidence that ^{18}F -flortaucipir binds to neuromelanin and melanin-containing cells (3,18), iron (19), monoamine oxidase B inhibitors (20), and vascular structures (21), to name a few. It is also a possibility that binding could be related to a yet-to-be-identified pathologic lesion or process that may or may not vary in burden by regions in PSP and CBD.

The comprehensive analyses, including modeling the relationships with and without partial-volume correction, excluded the likelihood that our results were influenced by volume loss. Other strengths to our study include the large number of autopsy-confirmed cases with a 4R tauopathy that had antemortem ^{18}F -flortaucipir and that all underwent semi-quantitative scoring by a single neuropathologist with over 30 y of experience with PSP and CBD pathology. Limitations include the fact that a quantitative histologic measure was not used, although semiquantitative scales were also used in the recent international study of the distribution patterns of tau pathology in PSP, which was performed with the intent to inform tau-neuroimaging distribution patterns (22). Other limitations are that the distribution of lesion severity within regions of interest—and the fact that the histologic region of interest represents a small sampled area within the larger ^{18}F -flortaucipir region of interest—could have impacted the ability to detect correlations. Furthermore, PET SUVRs can be influenced by different biologic and technical factors (23).

CONCLUSION

The results of this study do not support differential affinity of ^{18}F -flortaucipir for any histologic lesion, including threads, in 4R tauopathies.

DISCLOSURE

This study was funded by NIH grants RF1-NS112153, R01-DC12519, R01-NS89757, and R01-DC14942. Val Lowe serves on the scientific advisory board of AVID Radiopharmaceuticals. No other potential conflict of interest relevant to this article was reported.

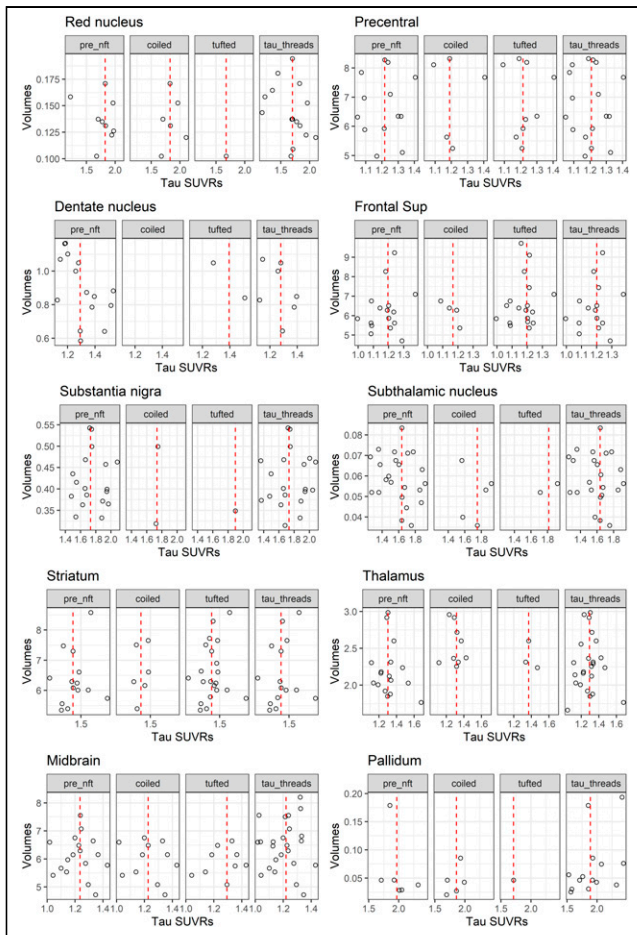


FIGURE 4. Scatterplots showing relationship between tau SUVR and volume across regions in cases that had frequent lesion counts (score = 3). Red dashed line represents median tau SUVR. nft = neurofibrillary tangles.

ACKNOWLEDGMENT

We acknowledge the Mayo ADIR Laboratory for PET processing pipelines.

KEY POINTS

QUESTION: Is ^{18}F -flortaucipir uptake in 4R tauopathies related to histologic lesion type?

PERTINENT FINDINGS: In this PET pathologic study of 29 autopsied patients who underwent ^{18}F -flortaucipir PET while alive and later died with autopsy-confirmed PSP or CBD, we semiquantified histologic lesion types in multiple brain regions and looked for associations between ligand uptake and lesion type using linear regression. We found only 2 weak associations.

IMPLICATIONS FOR PATIENT CARE. There is little evidence linking ^{18}F -flortaucipir uptake to any one lesion type in 4R tauopathies. Hence, other factors must be considered when designing second and third generations of 4R tau PET ligands.

REFERENCES

- Dickson DW, Bergeron C, Chin SS, et al. Office of Rare Diseases neuropathologic criteria for corticobasal degeneration. *J Neuropathol Exp Neurol.* 2002;61:935–946.
- Hauw JJ, Daniel SE, Dickson D, et al. Preliminary NINDS neuropathologic criteria for Steele-Richardson-Olszewski syndrome (progressive supranuclear palsy). *Neurology.* 1994;44:2015–2019.
- Lowe VJ, Curran G, Fang P, et al. An autoradiographic evaluation of AV-1451 tau PET in dementia. *Acta Neuropathol Commun.* 2016;4:58.
- Xia CF, Arteaga J, Chen G, et al. [^{18}F]T807, a novel tau positron emission tomography imaging agent for Alzheimer's disease. *Alzheimers Dement.* 2013;9:666–676.
- Whitwell JL, Lowe VJ, Tosakulwong N, et al. [^{18}F]AV-1451 tau positron emission tomography in progressive supranuclear palsy. *Mov Disord.* 2017;32:124–133.
- Josephs KA, Whitwell JL, Tacik P, et al. [^{18}F]AV-1451 tau-PET uptake does correlate with quantitatively measured 4R-tau burden in autopsy-confirmed corticobasal degeneration. *Acta Neuropathol (Berl).* 2016;132:931–933.
- McMillan CT, Irwin DJ, Nasrallah I, et al. Multimodal evaluation demonstrates in vivo ^{18}F -AV-1451 uptake in autopsy-confirmed corticobasal degeneration. *Acta Neuropathol (Berl).* 2016;132:935–937.
- Ghirelli A, Tosakulwong N, Weigand SD, et al. Sensitivity-specificity of tau and amyloid beta positron emission tomography in frontotemporal lobar degeneration. *Ann Neurol.* 2020;88:1009–1022.
- Montine TJ, Phelps CH, Beach TG, et al. National Institute on Aging-Alzheimer's Association guidelines for the neuropathologic assessment of Alzheimer's disease: a practical approach. *Acta Neuropathol (Berl).* 2012;123:1–11.
- Josephs KA, Mandrekar JN, Dickson DW. The relationship between histopathological features of progressive supranuclear palsy and disease duration. *Parkinsonism Relat Disord.* 2006;12:109–112.
- Whitwell JL, Ahlskog JE, Tosakulwong N, et al. Pittsburgh compound B and AV-1451 positron emission tomography assessment of molecular pathologies of Alzheimer's disease in progressive supranuclear palsy. *Parkinsonism Relat Disord.* 2018;48:3–9.
- Ewert S, Pletting P, Li N, et al. Toward defining deep brain stimulation targets in MNI space: a subcortical atlas based on multimodal MRI, histology and structural connectivity. *Neuroimage.* 2018;170:271–282.
- Schwarz CG, Thorneau TM, Weigand SD, et al. Selecting software pipelines for change in flortaucipir SUVR: balancing repeatability and group separation. *Neuroimage.* 2021;238:118259.
- Jack CR Jr, Wiste HJ, Weigand SD, et al. Defining imaging biomarker cut points for brain aging and Alzheimer's disease. *Alzheimers Dement.* 2017;13:205–216.
- Schwarz CG, Tosakulwong N, Senjem ML, et al. Considerations for performing level-2 centiloid transformations for amyloid PET SUVR values. *Sci Rep.* 2018;8:7421.
- Zhang W, Tarutani A, Newell KL, et al. Novel tau filament fold in corticobasal degeneration. *Nature.* 2020;580:283–287.
- Tarutani A, Miyata H, Nonaka T, et al. Human tauopathy-derived tau strains determine the substrates recruited for templated amplification. *Brain.* 2021;144:2333–2348.
- Marquie M, Normandin MD, Vanderburg CR, et al. Validating novel tau positron emission tomography tracer [F-18]-AV-1451 (T807) on postmortem brain tissue. *Ann Neurol.* 2015;78:787–800.
- Choi JY, Cho H, Ahn SJ, et al. Off-target ^{18}F -AV-1451 binding in the basal ganglia correlates with age-related iron accumulation. *J Nucl Med.* 2018;59:117–120.
- Vermeiren C, Motte P, Viot D, et al. The tau positron-emission tomography tracer AV-1451 binds with similar affinities to tau fibrils and monoamine oxidases. *Mov Disord.* 2018;33:273–281.
- Saint-Aubert L, Lemoine L, Chiotis K, Leuzy A, Rodriguez-Vieitez E, Nordberg A. Tau PET imaging: present and future directions. *Mol Neurodegener.* 2017;12:19.
- Kovacs GG, Lukic MJ, Irwin DJ, et al. Distribution patterns of tau pathology in progressive supranuclear palsy. *Acta Neuropathol (Berl).* 2020;140:99–119.
- Adams MC, Turkington TG, Wilson JM, Wong TZ. A systematic review of the factors affecting accuracy of SUV measurements. *AJR.* 2010;195:310–320.